Society For Biomaterials

In vitro degradation, biocompatibility, and *in vivo* osteogenesis of poly(lactic-*co*-glycolic acid)/calcium phosphate cement scaffold with unidirectional lamellar pore structure

Fupo He,[1] Jiandong Ye[1,2]

[1]School of Materials Science and Engineering, South China University of Technology, Guangzhou 510641, China
[2]National Engineering Research Center for Tissue Restoration and Reconstruction, Guangzhou 510006, China

Received 20 February 2012; revised 20 April 2012; accepted 7 May 2012
Published online 00 Month 2012 in Wiley Online Library (wileyonlinelibrary.com). DOI: 10.1002/jbm.a.34265

Abstract: The aim of this study was to investigate the *in vitro* degradation, cytocompatibility, and *in vivo* osteogenesis of poly(lactic-*co*-glycolic acid) (PLGA)/calcium phosphate cement (CPC) scaffold with unidirectional lamellar pore structure. CPC-based scaffold was fabricated by unidirectional freeze casting, and PLGA was used to improve the mechanical properties of the CPC-based scaffold, which covered the surface of the pore wall as coating. The *in vitro* degradation results demonstrated that the PLGA/CPC scaffold had good degradability. The degradation of PLGA film on the surface of the scaffold made the CPC matrix exposed, which facilitated cell response and osteogenesis. Rat bone mesenchymal stem cells (rMSCs) were seeded on the PLGA/CPC composite scaffold. Cell viability, proliferation, and differentiation on the PLGA/CPC composite scaffold were evaluated. The results showed that viable rMSCs attached on the surface of pore wall gradually penetrated into the internal pores of the scaffold as prolongation of culture time. In addition, the rMSCs seeded on the scaffold exhibited good proliferation and growing alkaline phosphatase activity. The scaffold was implanted in the defects in distal end of femora of New Zealand white rabbits. Histological evaluation indicated that the PLGA/CPC scaffold with unidirectional lamellar pore structure had good biocompatibility and effective osteogenesis. These results suggest PLGA/CPC composite scaffold with unidirectional lamellar pore structure is a promising scaffold for bone tissue engineering. © 2012 Wiley Periodicals, Inc. J Biomed Mater Res Part A: 00A:000–000, 2012.

Key Words: scaffold, calcium phosphate cement, PLGA, unidirectional lamellar pore, degradation, cytocompatibility, osteogenesis

How to cite this article: He F, Ye J. 2012. *In vitro* degradation, biocompatibility, and *in vivo* osteogenesis of poly(lactic-*co*-glycolic acid)/calcium phosphate cement scaffold with unidirectional lamellar pore structure. J Biomed Mater Res Part A 2012:00A:000–000.

INTRODUCTION

Tissue engineering is considered as a promising strategy to heal bone defects caused by trauma or disease.[1,2] Scaffold plays an important role in bone tissue engineering by providing a temporary three-dimensional (3D) template to guide ingrowth of cells and bone tissue, and transporting essential nutrients and waste products. Ideal scaffold should be biocompatible, osteoconductive, and have high porosity and interconnected macroporous structure for cell adhesion, migration, and proliferation. Moreover, enough mechanical strength is required to support tissue structure after implantation.[3,4]

Unidirectional freeze casting has been used in polymers and inorganic materials [collagen, hydroxyapatite, poly(lactic-*co*-glycolic acid) (PLGA), etc.] to fabricate scaffolds with unidirectional pore structure.[5–7] The porosity, pore size, and mechanical strength can be controlled by varying the cryogenic temperature and concentration of materials. Many researches revealed that the unidirectional pore structure facilitated cell growth into internal pores.[8–10]

Calcium phosphate (CaP) materials such as hydroxyapatite (HA), β-tricalcium phosphate, and bioactive glass, are recognized as preferable materials for bone tissue engineering scaffold.[11] Biocompatibility and osteoconductivity are the main advantages of CaP scaffolds because of their chemical similarities to the inorganic component of natural bone,[12] which supports the growth of bone cells and makes the implant bond strongly with peripheral tissues.[13–16] However, some drawbacks such as relatively low degradation rate, low mechanical strength, and high brittleness hinder the use of CaP scaffolds. The main reason for slow degradation of CaP ceramics is that the manufacture of bioceramics is the process of thermal treatment or sintering,

Correspondence to: J. Ye; e-mail: jdye@scut.edu.cn
Contract grant sponsor: National Natural Science Foundation of China; contract grant number: 51172074
Contract grant sponsor: National Basic Research Program of China; contract grant number: 2012CB619100

which would greatly increase the grain size and crystallinity of the CaP ceramics.[17]

As a self-setting biomaterial, calcium phosphate cement (CPC) has been proved to be extremely biocompatible and osteoconductive, as demonstrated by the fast deposition of new bone on the cement surface.[18,19] The formation of hardened CPC structure is acquired by hydration reaction at body or room temperature, dispensing with sintering at high temperature. The crystalline product forms through dissolution-precipitation reaction, and the final product of setting reaction of CPC usually is poorly crystalline HA, which is more chemically similar to natural bone apatite. Because of its poor crystallinity and microporous structure, CPC is faster degradable than sintered CaP bioceramics. CPC, unlike sintered bioceramics, is easy to shape as required form during the operation. These advantages make CPC a promising material for bone tissue engineering scaffold.

However, poor mechanical strength is a shortcoming for CPC scaffold as well as other CaP ceramic scaffolds. Improvement of mechanical properties of inorganic scaffolds can be achieved by composite preparation with polymers.[20–22] PLGA as a synthetic polymer has been approved by FDA to be widely used as implantable screws, pins, drug delivery devices, and tissue engineering scaffolds because of its biocompatibility, biodegradability, and processibility.[23,24] The specific physical and chemical characteristics (degradation rate, mechanical properties, etc.) of PLGA can be controlled by varying its composition and molecular weight.[25,26] PLGA coating on the surface of inorganic scaffolds can significantly improve the compressive strength and toughness of the inorganic scaffolds.[27–29]

In this study, we investigated the *in vitro* degradation, cytocompatibility and *in vivo* osteogenesis of the PLGA/CPC composite scaffold with unidirectional lamellar pore structure. rMSCs were cultured on the scaffold, and Live/Dead assay, water-soluble tetrazolium-8 (WST-8) assay, and alkaline phosphatase (ALP) activity were used to evaluate cell viability, proliferation, and differentiation on the scaffold constructs. The scaffolds were implanted in the defects in distal end of femora of New Zealand white rabbits to observe the bone formation in PLGA/CPC scaffold.

MATERIALS AND METHODS

Materials

The CPC powder used in this study was prepared by mixing partially crystallized calcium phosphate (PCCP, median diameter of 16.5 μm) and dicalcium phosphate anhydrous (DCPA, median diameter of 3.7 μm) at a weight ratio of 1:1, as described in our previous work.[30,31] PCCP was synthesized from an aqueous solution of $Ca(NO_3)_2{\cdot}4H_2O$ (0.36 mol/L) and $(NH_4)_2HPO_4{\cdot}12H_2O$ (0.15 mol/L) by chemical precipitation method in our laboratory. The deposits were centrifugally separated, freeze-dried, and calcined at 450°C for 2 h in a furnace to partially crystallize. The as-calcined PCCP powders were milled in a planetary mill using ZrO_2 balls at 400 rpm for 2 h. DCPA was commercially obtained from the Shanghai No. 4 Reagent & H. V. Chemical, China. Sodium alginate (SA) as setting accelerator was purchased from Tianjin Fuchen Chemical Reagent, China. PLGA (75/25 lactide to glycolide ratio, MW: 100,000, the inherent viscosity of 1.39 dL/g) was purchased from Jinan Daigang Biomaterials, China. Cell-culture related reagents were purchased from Gibco (Invitrogen) except specialized.

Preparation of PLGA/CPC scaffold

The method for fabrication of PLGA/CPC scaffolds was described in our previous work.[29] The SA was dissolved in deionized water to prepare 2 wt % (W/V) SA solution, which was used as cement liquid. The CPC slurry was prepared by mixing the SA solution with the CPC powder at the liquid to CPC powder (L/P) ratio of 3.25 mL/g. Then the slurry was poured into cylindrical glass tubes (with an inner diameter of 7 mm and a height of 14 mm) and immediately put on a cold plane to freeze. Temperature difference from bottom (at −30°C) to top (at room temperature) of slurry in the glass tubes caused the ice orientationally crystallized. The frozen samples were freeze dried for 48 h to obtain the unidirectional pores. Dense PLGA/CPC composites without macropores were fabricated to be used as control. In brief, CPC/SA mixture was mixed with deionized water at the liquid/powder ratio of 0.4 mL/g, and the paste was put into the steel mold, and then demoulded, dense CPC blocks without macropores were obtained. The CPC scaffolds and dense CPC blocks were incubated in a humidor with 98% relative humidity at 37°C for 2 days at least to make sure sufficient setting reaction of CPC. The hydrated CPC scaffolds and dense CPC blocks were dried in an oven at 50°C for 24 h. PLGA was dissolved in dichloromethane (CH_2Cl_2) at the fraction of 0.20 g/mL (W/V) to form a flowable solution. The CPC scaffolds and dense CPC blocks were immersed into the PLGA solution, followed by vacuum infiltration for 5 h. PLGA was infiltrated into the pores of scaffolds under the pressure difference, and most CH_2Cl_2 were eliminated under the low vacuum. After infiltration procedure, the samples were dried in the air for at least 48 h to eliminate the rest of CH_2Cl_2. Finally, PLGA/CPC scaffolds and dense PLGA/CPC samples were obtained for assessments.

Scaffold characterization

The morphology of composite scaffolds was observed by an environmental scanning electron microscope (Quanta 200, FEI, The Netherlands) and a field emission scanning electron microscope (Navo NanoSEM 430, FEI, The Netherlands). After being dried, the composite scaffold samples were mounted on an aluminium stub by carbon tape and sputtered with gold. An accelerating voltage of 2–15 kV was used to characterize the morphology of the composite scaffolds.

The compressive strength of cylindrical scaffolds (diameter = 7 mm, height = 12 mm) was measured using a universal material testing machine (Instron 5567, Instron, Britain) at a crosshead speed of 0.5 mm/min. Each measurement was repeated for six times and the average value was calculated.

In vitro degradation

In vitro degradation evaluation of the porous scaffolds was performed in phosphate buffered saline (PBS) solution at pH 7.2 and 37°C under mechanical vibration at a speed of 120 rpm with an orbital shaker. The PLGA/CPC scaffold specimens were weighed and then immersed in polystyrene bottles containing PBS solution (the ratio of solution to sample: 50 mL/g) for up to 12 weeks. Three-fourths of PBS solution in the bottles was replaced with fresh PBS solution every week. The pH value of the PBS solution was measured with a pH meter (PHS-2C, Jingke, Shanghai, China) at intervals. The samples were collected every 2 weeks, washed, and air-dried. The dried specimens were used for measurement of compressive strength and weight loss (WL), and microstructural characterization of the scaffolds. The WL was calculated as follows:

$$WL\ \% = W_0 - W_d/W_0 \times 100\%$$

where W_0 represents the initial weight of the scaffold samples and W_d denotes the weight of the dried specimens after degraded for different time. Each measurement was performed six times and the average value was calculated.

Rat bone marrow mesenchymal stem cells (rMSCs) harvest

rMSCs were obtained from bilateral femora of Fischer 344/N syngeneic rats. Both femora were cut away from the epiphysis of the rat. Bone marrow was flushed out of marrow cavity with 15 mL of culture medium minimal essential medium eagle (MEME) containing 10% fetal bovine serum (FBS) and 1% antibiotics (100 U/mL penicillin G, 100 μg/mL streptomycin sulfate, and 0.25 μg/mL amphotericin B). The bone marrow suspension was transferred into a 75 cm^2 tissue culture polystyrene flask and incubated at 37°C in a humidified incubator with 5% CO_2. The culture medium was refreshed every 3 days to remove dead cells and wastes produced by metabolism of cells. After about 90% confluence was reached, the rMSCs were passaged.

Cell culture and cell seeding

The PLGA/CPC scaffolds and dense PLGA/CPC blocks were cut into disks with 7 mm in diameter and 2.5 mm in height. After being sterilized by gamma radiation (15 kGy), the disks were put into 24-well plates and pre-wetted in MEME solution for 12 h. rMSCs at passage 1 were used. For assays of cell viability and cell proliferation, 35 μL of cell suspension (10^6 cells/mL) was seeded onto the surface of the samples in 24-well plates. The cell-seeded samples were incubated at 37°C in a humidified incubator with 5% CO_2 for 2 h to allow the cells to adhere onto the sample surface, then 1 mL of culture medium was added to each well to cover the samples. The culture medium was replaced with fresh one every 3 days.

Cell viability

The viability of rMSCs cultured on scaffolds was evaluated using a Live/Dead kit (Biotium) according to standard protocol provided by the manufacturer after 1, 3, and 7 days' culture. Only "Live" assay was performed in this study. The cell-sample constructs were washed with PBS and incubated in standard working solution at 37°C for 45 min. After being washed with PBS solution twice, the constructs were observed with a fluorescence microscope (Zeiss Axioskop 40, Germany). After observation of scaffold surface was completed, the scaffold constructs were cut along the direction parallel to the pore orientation to observe the penetration of rMSCs into the internal pores.

Cell proliferation

Cell proliferation was evaluated by WST-8 assay using a CCK-8 kit (Dojindo Laboratories, Japan) according to the manufacturer's instructions. The cell-sample constructs were transferred to a new cell culture plate on day 1, 3, and 7, respectively. 1 mL of MEME solution was added to each well of plate, followed by addition of 100 μL of CCK-8 reagent. After incubation at 37°C for 2 h, 100 μL of upper solution was pipetted to a 96-well plate. The absorbance at 450 nm was measured with enzyme linked immunosorbent assay reader. The optical density value was normalized to the number of rMSCs.

Cell differentiation

40 μL of cell suspension (2.5×10^6 cells/mL) was seeded onto the samples in 24-well plate. After 2 h, 1 mL of culture medium (MEME supplemented with 10% FBS, 10 m*M* sodium β-glycerophosphate, 10 n*M* dexamethasone, and 82 mg/mL vitamin C) was added to the wells. The cell-constructs were cultured in a humidified atmosphere of 5% CO_2 at 37°C. After cultured for 7 and 14 days, the cell-constructs were washed twice with PBS solution. An aliquot of 400 μL of 0.05% Triton X was added to the culture well and the mixture was incubated at 4°C for 2 h. The supernatant was tested for intracellular total protein content and ALP activity. Total protein content was assayed by the Bradford method using a Bio-Rad protein assay reagent kit (Bio-Rad Laboratories, Japan) according to the manufacturer's instructions. The total protein content was determined by measuring the absorbance at 595 nm. The ALP activity of the rMSCs was assayed using a Laboassay™ ALP kit (Wako Pure Chemicals, Japan) in accordance with the manufacturer's instructions. 20 μL of supernatant was incubated with 100 μL of *p*-NPP solution (*p*-nitrophenyl phosphate solution) at 37°C, after 15 min, 80 μL of NaOH solution was added to terminate the reaction. The amount of *p*-NP (*p*-Nitrophenol) was estimated by measuring the absorbance at 405 nm.

Histological evaluation

12 healthy New Zealand white rabbits, with an average weight of 3.0 kg, were used for implantation of PLGA/CPC scaffolds. After being anesthetized with pentobarbital sodium under sterile condition, a critical size defect (Φ6 × 11 mm) was made in the distal end of the femur. The PLGA/CPC scaffold constructs with the size of Φ6 × 11 mm were implanted into the defects in the rabbit femora.

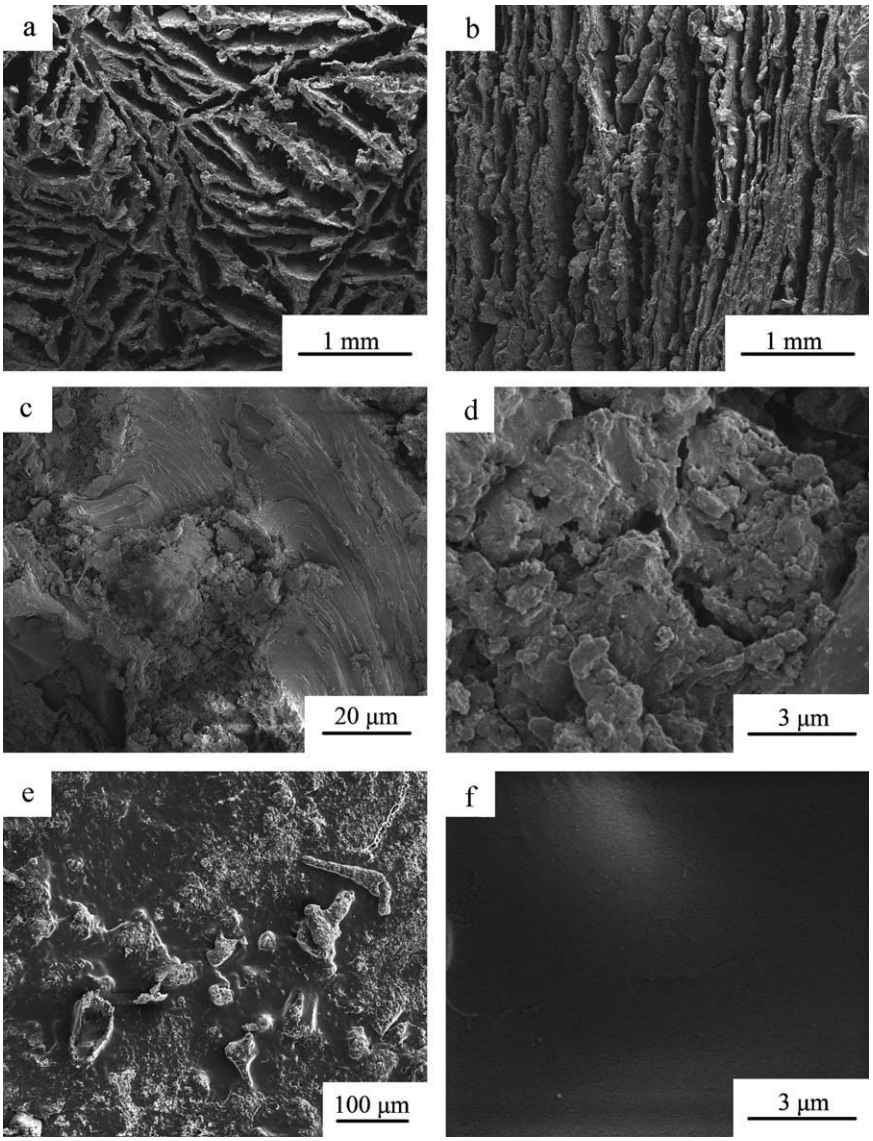

FIGURE 1. SEM micrographs of PLGA/CPC scaffold under different magnifications. (a, c, d) represent the cross section perpendicular to the long axis of the cylindrical sample, (b) represents the cross section parallel to the long axis of the cylindrical sample, and (e, f) represent the surface morphology of internal pore wall.

Bandage was used to fix the implanted site of femur. Rabbits were killed at 4, 8, and 16 weeks after implantation. The samples together with surrounding tissue were excised, fixed in 10% neutral buffered formalin, decalcified, and embedded in paraffin. Tissue blocks were sectioned to 5 μm in thickness and stained with hematoxylin and eosin, and observed with a light microscope (Axioskop 40, Zeiss, Germany).

Statistics/data analysis

All data points are an average of at least three replicates and expressed as mean ± standard deviation. Statistical comparisons were performed by one-way analysis of variance for multiple comparisons. Statistical significance for $p < 0.05$ and $p < 0.01$ were denoted by * and **, respectively.

RESULTS

Scaffold characterization

The compressive strength of the PLGA/CPC scaffold was 5.44 ± 0.53 MPa; the apparent porosity of the PLGA/CPC scaffold was 58.50% ± 2.50%, which was determined according to the method described in the reference.[32] Figure 1 shows the morphology and microstructure of the PLGA/CPC composite scaffold. Lamellar macropores were observed at the cross section perpendicular to the direction of long axis of the cylindrical sample. The width of macropores were in the range of 100–200 μm, while the length were larger than 500 μm [Fig. 1(a)]. Highly unidirectional macropores with 100–200 μm width were observed from the cross section parallel to the long axis of the cylindrical sample [Fig. 1(b)]. Figure 1(c,d) exhibit the cross-sectional

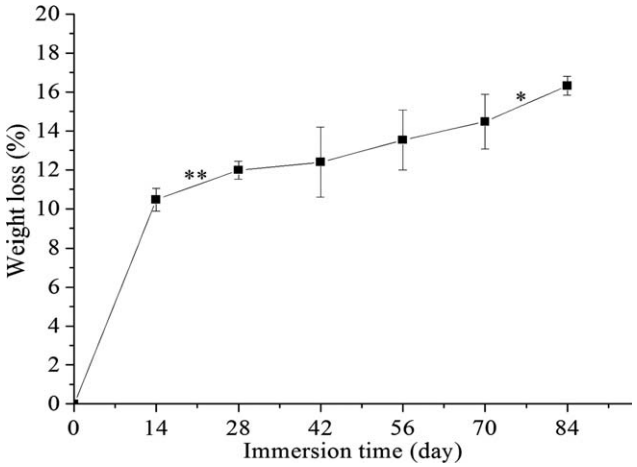

FIGURE 2. Weight loss of the PLGA/CPC scaffold as a function of immersion time.

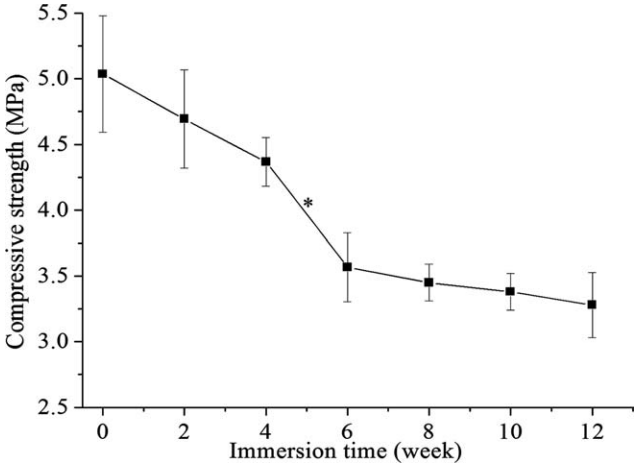

FIGURE 4. Compressive strength versus immersion time curve of the PLGA/CPC scaffold.

morphology of the composite scaffold with higher magnifications. CPC matrix was covered by thin PLGA film. Figure 1(e,f) clearly show that PLGA film covered the surface of internal pore wall of the composite scaffold, and CPC matrix was hardly exposed on the surface.

In vitro degradation behavior

The WL of the PLGA/CPC composite scaffold as a function of immersion time is shown in Figure 2. After immersion in PBS solution for 2 weeks, the percentage of WL of scaffold was 10.47% ± 0.58%, the WL of scaffold gradually increased as immersion time prolonged. However, the increment of WL after immersed for longer time was not so significant compared with that after immersed for 2 weeks. After immersion in PBS solution for 12 weeks, the WL of scaffold was only 16.31% ± 0.48%.

The pH variation of PBS solution as a function of immersion time is exhibited in Figure 3. pH value gradually decreased during immersion in PBS solution at the early stage, and then increased after immersion for 3 weeks; finally, it reached 7.28 after immersion for 12 weeks.

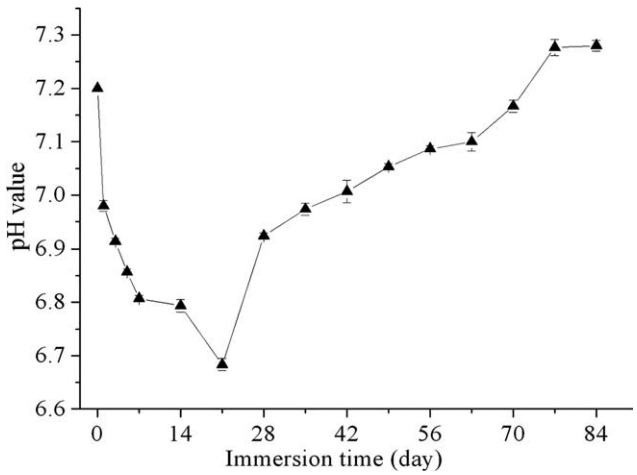

FIGURE 3. Variation of pH value of the PBS solution during *in vitro* degradation of the PLGA/CPC scaffold.

The compressive strength versus the degradation time curve of the PLGA/CPC scaffold is illustrated in Figure 4. It is notable that the compressive strength decreased with prolongation of immersion time. The compressive strength of the scaffold decreased from 5.04 ± 0.44 MPa without immersion (or at 0 week) to 4.69 ± 0.37 MPa after immersion for 2 weeks, and finally to 3.28 ± 0.25 MPa after immersion for 12 weeks.

The morphology of the PLGA/CPC scaffold after immersed in PBS solution for different time is presented in Figures 5 and 6. Figure 5 exhibits that the pore structure of the scaffold was not destroyed during immersion in PBS solution. The morphology of pore wall (Fig. 6) shows that the PLGA film covered on CPC matrix gradually degraded, accompanied by more and more exposure of CPC. After immersion for 4 weeks, the PLGA film was eroded and CPC was slightly exposed. After immersed in PBS solution for 12 weeks [Fig. 6(d,e)], the PLGA film on the surface of pore wall of the scaffold obviously degraded, and CPC matrix was obviously exposed while a certain amount of PLGA phase still remained to keep the scaffold integrity.

Cell viability

The viability of rMSCs cultured on the PLGA/CPC scaffold was evaluated by the use of Live/Dead assay after 1, 3, and 7 days' culture (Fig. 7). It is shown that a certain amount of rMSCs appeared on the surface of pore wall of the PLGA/CPC composite scaffold as well as the dense sample (control) on the 1st day [Fig. 7(a,b)]. As cultured for 3 days, the cell obviously increased on both samples [Fig. 7(c,d)]. After 7 days, the cell nearly fully covered the surface of the dense sample; however, unremarkable cell proliferation was observed on the outer surface of the scaffold [Fig. 7(e,f)]. To watch if the cell migrated into the interior of the scaffold, the scaffold was cut along the pore orientation of the scaffold. Scarcely any cell can be observed in the internal unidirectional macropores on the 3rd day [Fig. 7(g)]. However,

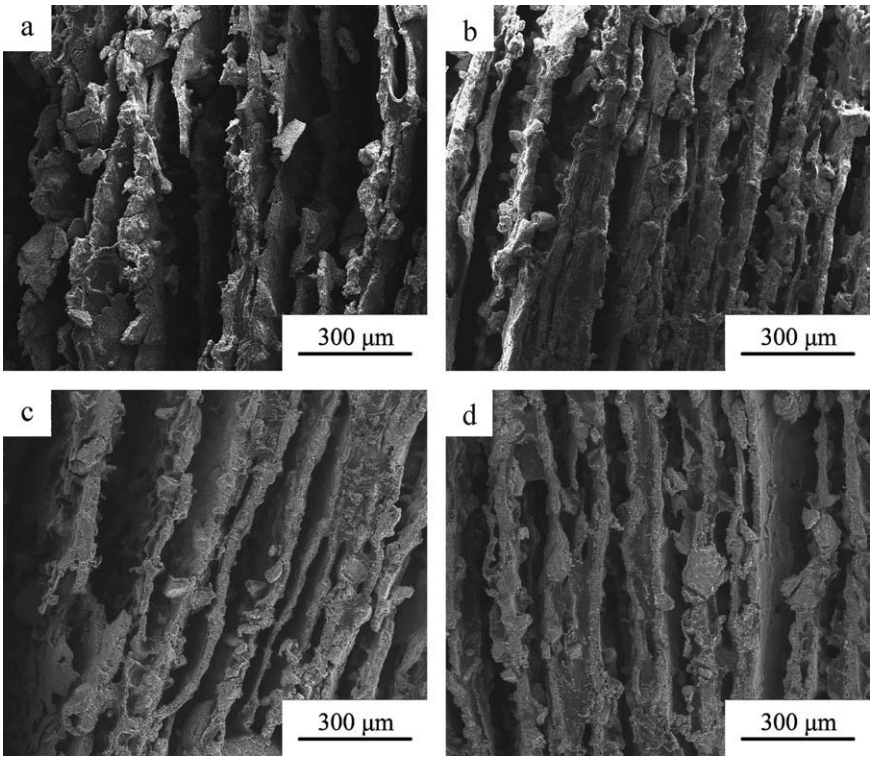

FIGURE 5. SEM images of the PLGA/CPC composite scaffold after immersion in PBS solution for 0 week (a), 4 weeks (b), 8 weeks (c), and 12 weeks (d).

a certain amount of cells can be observed in the internal pores of scaffold after 7 days' culture [Fig. 7(h)]. These demonstrate that cell can migrate into the unidirectional lamellar pores of the scaffold.

Cell proliferation

The cell proliferation on the PLGA/CPC scaffold was analysed using WST-8 assay after 1, 3, and 7 days' culture [Fig. 8(a)]. It can be seen that the number of cells on the scaffold was significantly lower than that on the dense sample after 1 day, which indicated that fewer viable cells were seeded on the PLGA/CPC scaffold than that on the dense sample. As the culture time prolonged, the cells significantly increased on the scaffold as well as the dense sample. Figure 8(b) exhibits the cell growth rates on both samples on the 3rd day and the 7th day. The cell growth rate of scaffold was lower than that on the dense sample after 3 days' culture (63.10% $\pm$ 24.85% vs. 90.58% $\pm$ 7.30%). However, after 7 days, the growth rate on the scaffold became much higher than that on the dense sample (46.83% $\pm$ 20.63% vs. 29.87% $\pm$ 3.760%). These suggest that the PLGA/CPC scaffold has no cytotoxicity and the cells proliferate well in it.

ALP activity

ALP activity assay was used to evaluate cell differentiation on the scaffold. The ALP activity was evaluated using the *p*-NPP assay on the 7th and 14th day. The ALP activity was normalized to the intracellular total protein. Figure 9 shows the intracellular total protein contents on the scaffold and the dense sample. The intracellular total protein content on the scaffold was higher than that on the dense sample on the 7th day. After 14 days, the total protein contents on both samples increased while the total protein content on scaffold was much higher than that on dense sample. These indicate that the cells on the scaffold were more than that on the dense sample on the 7th and 14th day. As shown in Figure 10, on day 7, the ALP production from rMSCs on the scaffold was significantly less than that on the dense sample. After 14 days, the cells on both samples exhibited significantly higher ALP activity than those after 7 days, nevertheless, the ALP activity of cells on scaffold was still markedly lower than that on the dense sample.

Histological evaluation

The histological evaluation results of the PLGA/CPC scaffold implanted in the defects of rabbit femora for 4, 8, and 16 weeks are shown in Figure 11. After 4 weeks' implantation [Fig. 11(a,b)], the PLGA/CPC scaffold was surrounded by host bone tissue, and the interface between the scaffold implant and the host bone tissue was clearly visible. A small part of the scaffold material degraded from the edge of the implant and was replaced by new bone. Bone tissues newly formed on the periphery but did not yet penetrate into the center of the scaffold. After 8 weeks' implantation [Fig. 11(c,d)], the interface between the scaffold and host bone was unclear. Some new bone tissues regenerated and gradually penetrated into the internal macropores of the scaffold,

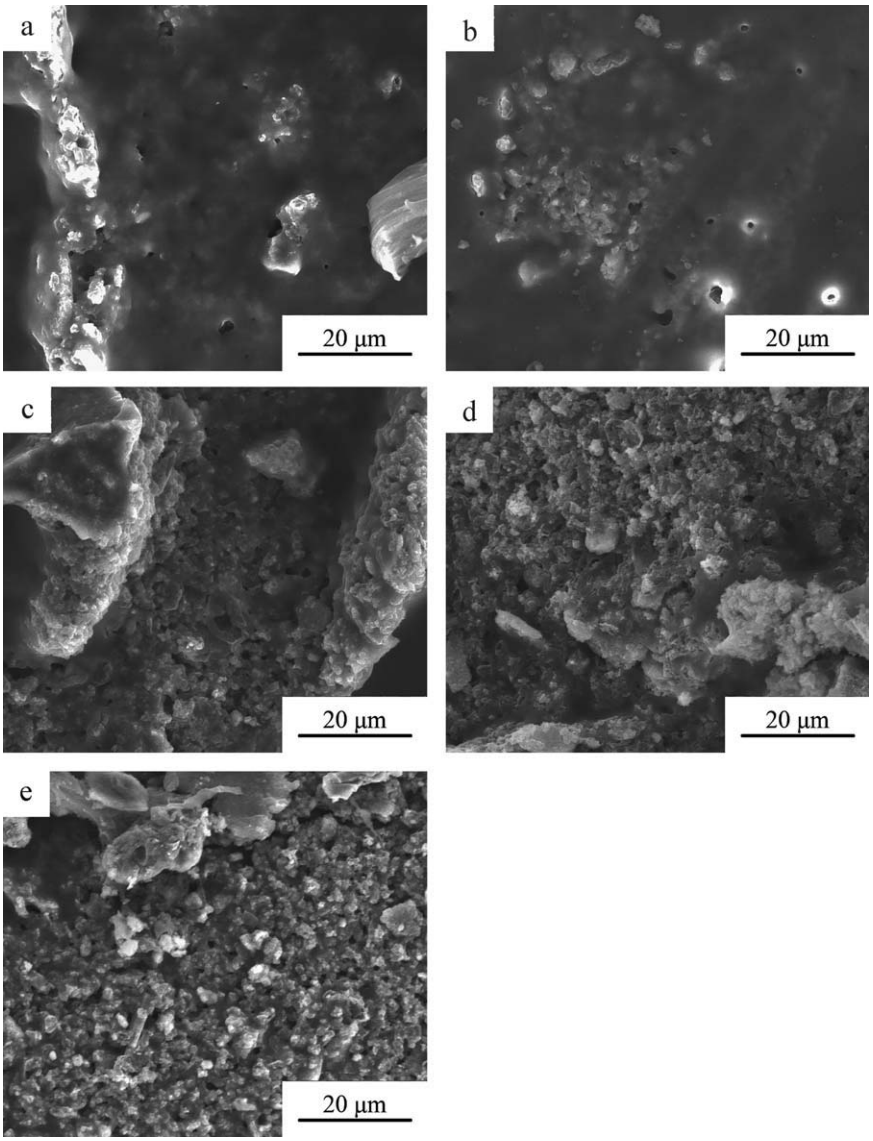

FIGURE 6. SEM images of the surface of macropore wall of the scaffold after immersion in PBS solution for 0 week (a), 4 weeks (b), 8 weeks (c), and 12 weeks (d) as well as the cross-sectional microstructure of PLGA/CPC composite scaffold after immersion in PBS solution for 12 weeks (e).

and a lot of osteoblasts were surrounded by the new bone tissues. After 16 weeks' implantation [Fig. 11(e,f)], new bone increasingly regenerated along the unidirectional macropores of scaffold, and numerous osteoblasts were observed in the new bone with the material residuals and fat cells close to the new bone.

DISCUSSION

Macropores with high interconnectivity facilitate the ingrowth of new bone tissue throughout the whole scaffold and improve bone reconstruction procedure. Many methods have been developed to introduce macropores into CPC, such as leaching out of soluble crystal, gas generation method using foaming agent, and air bubble trapping.[33–38] However, the interconnectivity of macropores is still a key issue for CPC scaffold.

Unidirectional freeze casting has been used for fabricating the scaffold with unidirectional pore structure and excellent interconnectivity. In previous study, we prepared highly interconnected CPC scaffold using unidirectional freeze casting.[29] PLGA was infiltrated into the CPC-based scaffold to obtain PLGA/CPC composite scaffold with better mechanical strength for bone repair. The compressive strength of the PLGA/CPC composite scaffold (5.44 MPa) was much higher than that of the pristine CPC scaffold (0.07 MPa). The compressive strength of the composite scaffold was comparable to that of cancellous bone, which shows a compressive strength of 2–12 MPa.[27] Polymer-based scaffold fabricated by unidirectional freeze casting obtains unidirectional tube-like pores, of which the size ranges from 20 to 200 μm.[7–9] However, the PLGA/CPC scaffold prepared using the same method in this work showed unidirectional lamellar

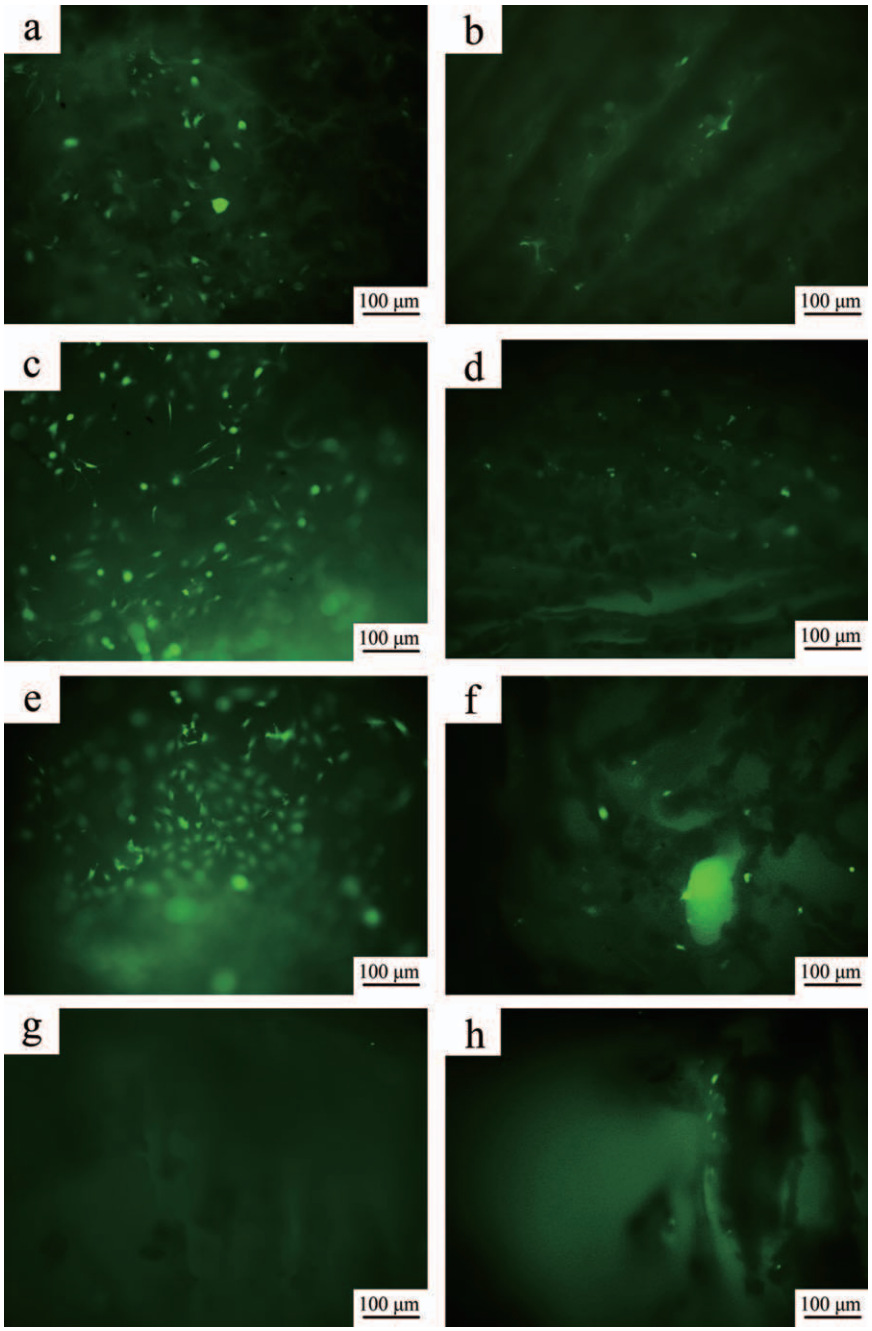

FIGURE 7. Fluorescence photographs of rMSCs on PLGA/CPC scaffold and dense sample (control) after 1 (a, b), 3 (c, d, and g) and 7 (e, f, and h) days' culture. (a, c, and e) represent the photographs of the dense sample, (b, d and f) denote the photographs of the PLGA/CPC scaffold, and (g, h) represent the photographs of interior of scaffold after 3 and 7 days' culture. [Color figure can be viewed in the online issue, which is available at wileyonlinelibrary.com.]

structure, and the width and length of the pores were larger than 100 μm and 500 μm, respectively, which can provide enough space for penetration of bone tissue and cells.[39]

In vitro degradation behavior of the PLGA/CPC scaffold in PBS solution at 37°C was investigated through characterizing the changes of weight, compressive strength, pH value, and pore morphology of the scaffold. The WL of scaffold increased as prolonging the immersion time. The change of pH value of PBS solution during immersion basically corresponded to the WL of the composite scaffolds. The WL of scaffold at 2 weeks reached 10.47% ± 0.58%, but after 2 weeks, the WL of the scaffold increased slowly. Correspondingly, pH value of PBS solution reached minimum at 3 weeks, then gradually increased to be close to the initial pH value. The main reasons are suggested to be: (1) the dissolution of CPC phase, which contained soluble salts;[26,27] (2) degradation of a part of PLGA with lower molecular weight, which existed in the PLGA with high average molecular

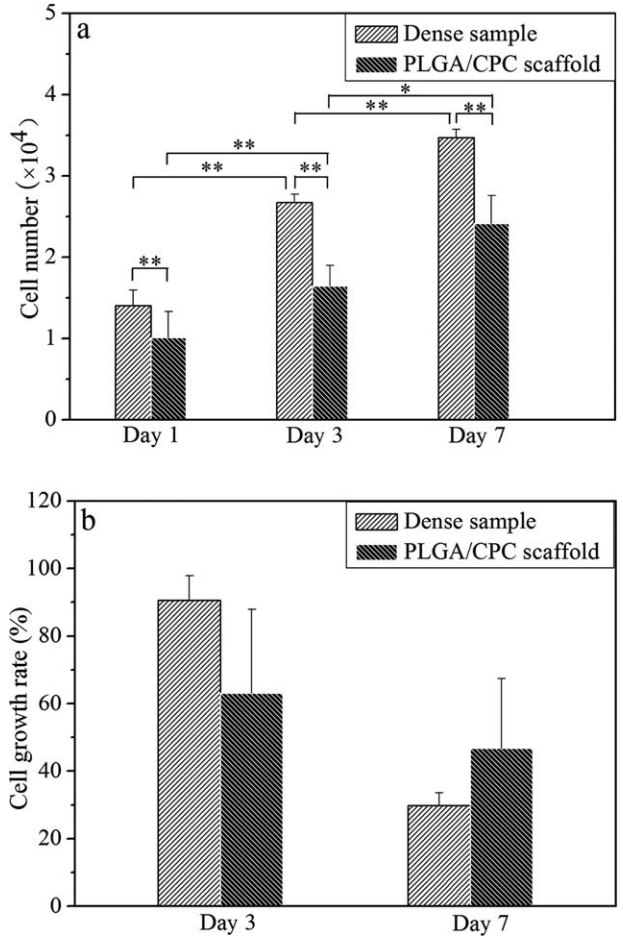

FIGURE 8. Proliferation of rMSCs on the PLGA/CPC scaffold and dense sample assessed by WST-8 assay (a). Cell growth rate on the scaffold and dense sample on the 3rd (against the 1st day) and the 7th (against the 3th day) day (b).

weight of 100,000. Taiyo et al.[40] reported that the degradability of PLGA sponges was dominated by autocatalyzed bulk degradation at the early stage, but by surface degradation at the late stage. Autocatalyzed bulk degradation can produce many small pores in the PLGA film and therefore increased the surface area, resulting in that the surface degradation had an edge over the autocatalyzed bulk degradation. Figure 6 exhibits that the surface morphology of pore wall did not markedly change after immersed for 4 weeks. But after 8 weeks, PLGA film obviously degraded and CPC matrix was partly exposed. The hydration product of CPC is poorly crystalline HA, which can promote cell response and osteogenesis. The degradation of CPC *in vivo* results from both dissolution and cellular activity of osteoclasts, macrophages, and white cells around the cement.[36] No cell-mediated resorption is involved during the degradation *in vitro*, so the degradation rate of scaffold *in vitro* is not comparable to that *in vivo*. Though the compressive strength of the scaffold decreases as the degradation proceeds, the strength will significantly increase once new bone start to grow into the macropores of scaffold after implantation.[41] Therefore, the mechanical strength is vital for a scaffold implant just at the early stage of implantation. With degradation of the PLGA film covered on the pore wall, more CPC directly contact with bone tissue and cells, which promotes ingrowth of new bone tissue and cells because of high osteoconductivity of porous CPC.

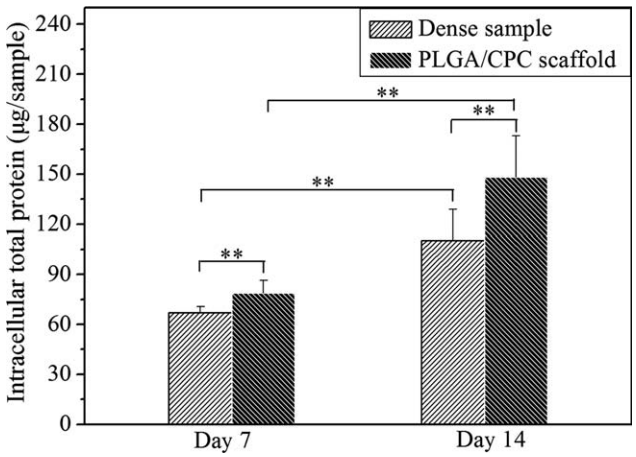

FIGURE 9. Intracellular total protein contents of rMSCs on the scaffold and dense sample after 7 and 14 days' culture.

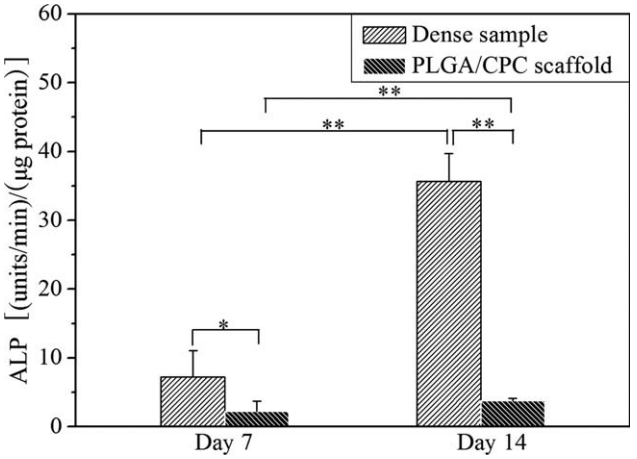

FIGURE 10. ALP activities of rMSCs on the PLGA/CPC scaffold and dense sample after 7 and 14 days' culture.

Live/Dead assay showed that rMSCs were present on the surface of pore wall of the PLGA/CPC scaffold. The cells on the surface of scaffold did not obviously increase after 7 days' culture compared to 3 days' culture. However, a certain amount of cells were clearly observed in the center of unidirectional pores of the scaffold after 7 days' culture, while rarely cells were inside the pores on the 3rd day. These demonstrate that cells are feasible to grow into internal pores of the scaffold.

The cell proliferation was evaluated using WST-8 assay. It was shown that cell number on the PLGA/CPC scaffold was notably lower than that on the dense sample after 1 day's culture. This revealed that the scaffold with unidirectional pore structure was not good for cell seeding. The scaffold with unidirectional pore structure meant that the

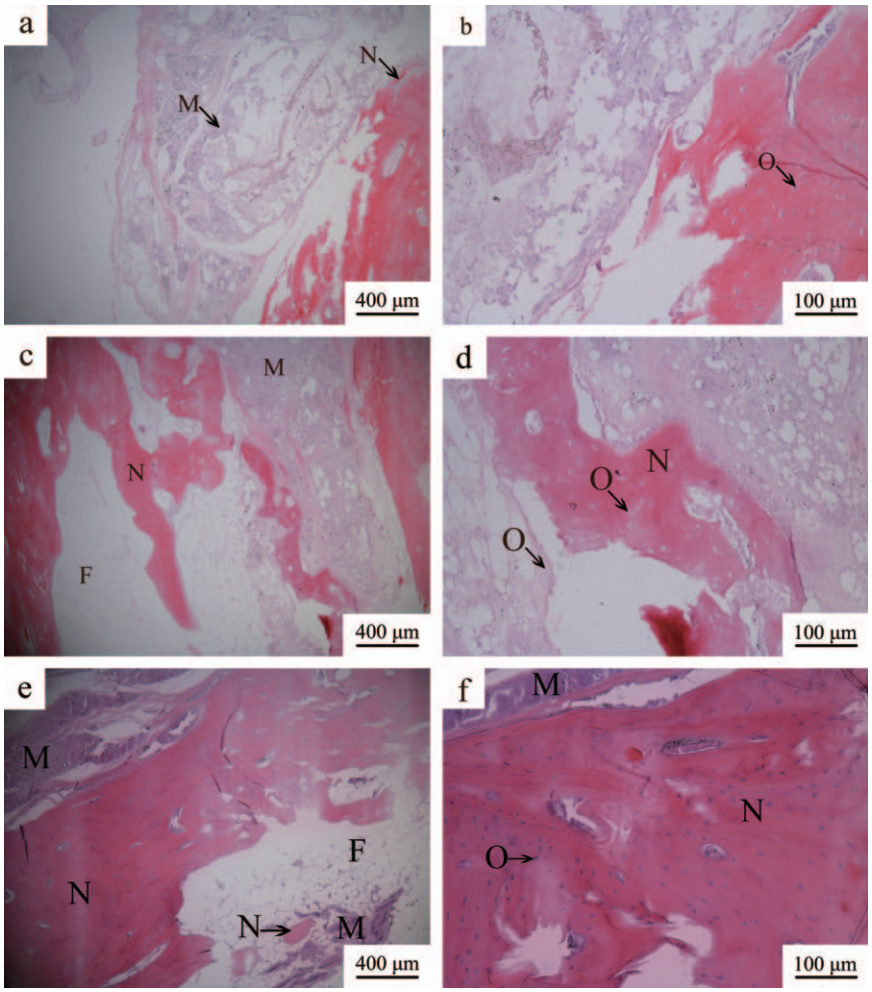

FIGURE 11. Histological evaluation of the PLGA/CPC scaffold implanted in bone defects of rabbit femora for 4 weeks (a, b), 8 weeks (c, d), and 16 weeks (e, f) under different magnifications. M, N, O, and F represent material residue, new bone tissue, osteoblast, and fat cell, respectively. [Color figure can be viewed in the online issue, which is available at wileyonlinelibrary.com.]

pore direction was parallel to the direction of gravity when conducting the cell culture. In this case, the cells were easy to fall onto the bottom of the wells of culture plate, resulting in that the cells attached on the surface of the scaffold were much less than that on the dense sample, which had horizontal surface for cell seeding. As prolongation of culture time, the cells proliferated on both samples. On the 3rd day, the cell growth rate on the scaffold was lower than that on the dense sample; however, after 7 days, the cell growth rate on scaffold was higher than that on the dense sample. The cell growth rate on the dense sample was inhibited because of limited surface area for further cell growth. The scaffold provided larger surface than the dense sample due to considerably higher porosity of the scaffold with macropores. The intracellular total protein content on both samples during the evaluation of ALP activity can be used to quantify the amount of rMSCs. The cell density for evaluation of ALP activity was much higher than that for cell viability and proliferation (10×10^4 vs. 3.5×10^4 cells/sample). According to fluorescent image [Fig. 7(e)], after 7 days, the cells nearly fully covered the surface of the dense sample which seeded with 3.5×10^4 cells. Thus, it can be inferred that the time for the cells fully grew on the surface of the dense sample, which seeded with 10×10^4 cells, would be much less than 7 days. In this case, it would be much earlier than 7th day when the cell growth rate was inhibited. Hence, the total protein content on the dense sample was much less than that on the scaffold on the 7th and 14th day. In other words, the scaffold owned greatly more cells than the dense sample on the 7th and 14th day. Based on these results, it is concluded that in fact the PLGA/CPC composite scaffold with unidirectional pore structure is beneficial for cell penetration and proliferation, although unfavorable for cell seeding.

ALP activity is regarded as an early marker of osteogenic differentiation during the *in vitro* experiment. In this study, the ALP activity of rMSCs on the scaffold was significantly lower than that on the dense sample on the 7th and 14th day, but the ALP activity of cells on the scaffold markedly increased as prolonging the culture time. The scaffold and dense sample were both composed of CPC and PLGA, for which the surface of CPC matrix was covered by PLGA

film [Fig. 1(e,f)]. These indicated that the composition and surface properties of both samples were similar. Therefore, the reason for the difference of ALP activity of cells on the scaffold and on the dense sample is the difference of their structures. The scaffold has much larger surface area for cell growth due to its macroporous structure and high porosity compared to the dense sample. The obvious difference of total protein contents between the scaffold and the dense sample confirmed this explanation. When the surface area is not enough for sustaining cell growth, the cells are feasible to form aggregation, which is liable to give rise to cell differentiation.[42] Therefore, the PLGA/CPC scaffold with unidirectional pore structure exhibited lower ALP activity. Even so, the ALP activity of the cells on the scaffold sustained growing as culture time prolonged.

Silva et al.[43] and Rose et al.[44] reported that combination of random and unidirectionally porous architectures enhanced cell and tissue infiltration throughout the HA scaffold. Chang et al.[45] found that cylindrical-type porous HA showed better osteoconductivity than sponge- and cross-type porous HA. But *in vivo* assessment of scaffold with unidirectional lamellar pore structure fabricated by unidirectional freeze casting was rarely reported. In this study, the PLGA/CPC composite scaffold with unidirectional lamellar pore structure was implanted in the defects in distal end of femora of New Zealand white rabbits to evaluate its osteogenesis. At the early stage of implantation, new bone regenerated and filled in the gap between the implant and the host bone, and the periphery of the scaffold, but no new bone was observed to penetrate into the center of the scaffold. As for the PLGA/CPC scaffold, PLGA film covered the surface of the porous CPC matrix. PLGA is biocompatible but has poor cell response and poor osteoconductivity.[32] When the PLGA film degraded gradually with prolonged time of implantation, much more exposed CPC matrix was beneficial for cell ingrowth and penetration of new bone tissue. Therefore, after 8 weeks' implantation, many osteoblasts and new bone tissue were detected inside the scaffold. After 16 weeks of implantation, plenty of new bone tissues inhabited the unidirectional macropores of the scaffold and the space produced by the degradation of PLGA and CPC matrix. All these results demonstrate that the scaffold with unidirectional lamellar pore structure is in favor of ingrowth of bone tissue and cells.

CONCLUSION

In vitro degradation, biocompatibility, and *in vivo* osteogenesis of the PLGA/CPC composite scaffold with unidirectional lamellar pore structure were evaluated in this study. The compressive strength of the composite scaffold decreased with the degradation of the scaffold, while CPC matrix was gradually exposed on the pore wall of the scaffold. The exposed CPC was more contributive to cell response and osteogenesis in comparison with the PLGA film coated on the pore wall of the scaffold. Although the unidirectional lamellar pore structure of the scaffold was unfavorable for cell seeding, it facilitated rMSCs ingrowth to the interior of the scaffold, and rMSCs proliferated well and gradually differentiated on the scaffold. Moreover, the results of *in vivo* implantation revealed the PLGA/CPC scaffold with unidirectional pore structure was beneficial for bone regeneration. Summarily, the PLGA/CPC composite scaffold with unidirectional pore structure possesses not only good biocompatibility but also good osteogenesis effect.

REFERENCES

1. Langer R, Vacanti JP. Tissue engineering. Science 1993;260: 920–926.2.
2. Mistry AS, Mikos AG. Tissue engineering strategies for bone regeneration. Adv Biochem Eng Biotechnol 2005;94:1–22.
3. Eggli PS, Muller W, Schenk CRK. Porous hydroxyapatite and tricalcium phosphate cylinders with two different pore size ranges implanted in the cancellous bone of rabbits. Clin Orthop Relat Res 1988;232:127–138.
4. Doblare M, Garcia JM, Gomez MJ. Modeling bone tissue fracture and healing: A review. J Eng Fract Mech 2004;71:1809–1840.
5. Fu Q, Rahaman MN, Dogan F, Bal BS. Freeze casting of porous hydroxyapatite scaffolds. I. processing and general microstructure. J Biomed Mater Res B Appl Biomater 2008;86:125–135.
6. Schoof H, Apel J, Heschel I, Rau G. Control of pore structure and size in freeze-dried collagen sponges. J Biomed Mater Res B Appl Biomater 2001;58:352–357.
7. Yang F, Qu X, Cui W, Bei J, Yu F, Lu S, Wang S. Manufacturing and morphology structure of polylactide-type microtubules orientation-structured scaffolds. Biomaterials;27:4923–4933.
8. Wilda H, Julie EG. Cell viability, proliferation and extracellular matrix production of human annulus fibrosus cells cultured within PDLLA/Bioglass® composite foam scaffolds in vitro. Acta Biomater 2008;4:230–243.
9. Wu X, Liu Y, Li X, Wen P, Zhang Y, Long Y, Wang X, Guo Y, Xing F, Gao J. Preparation of aligned porous gelatin scaffolds by unidirectional freeze-drying method. Acta Biomater 2010;6:1167–1177.
10. Yunoki S, Ikoma T, Tsuchiya A, Monkawa A, Ohta K, Sotome S, Shinomiya K, Tanaka J. Fabrication and mechanical and tissue ingrowth properties of unidirectionally porous hydroxyapatite/collagen composite. J Biomed Mater Res B Appl Biomater 2007;80:166–173.
11. Del Real RP, Ooms E, Wolke J, Vallet-Regi M, Jansen JA. In vivo bone response to porous calcium phosphate cement. J Biomed Mater Res 2003;65:30–36.
12. Rizzi SC, Heath DJ, Coombes AG, Bock N, Textor M, Downes S. Biodegradable polymer/hydroxyapatite composites: Surface analysis and initial attachment of human osteoblasts. J Biomed Mater Res 2001;55:475–486.
13. Wheeler DL, Stokes KE, Park HE, Hollinger JO. Evaluation of particulate bioglass in a rabbit radius ostectomy model. J Biomed Mater Res 1997;35:249–254.
14. Wheeler DL, Stokes KE, Hoellrich RG, Chamberland DL, McLoughlin SW. Effect of bioactive glass particle size on osseous regeneration of cancellous defects. J Biomed Mater Res 1998;41:527–533.
15. Hench LL, Splinter RJ, Allen WC, Greenlee TK. Bonding mechanism at the interface of ceramic prosthetic materials. J Biomed Mater Res 1971;5:117–141.
16. Hench LL. Bioceramics. J Am Ceram Soc 1998;81:1705–1728.
17. Vallet-Regí M, Gonz′alez-Calbet J. Calcium phosphates in the substitution of bone tissue. Prog Sol State Chem 2004;32:1–31.
18. Ooms EM, Wolke JGC, van der Waerden JPCM, Jansen JA. Trabecular bone response to injectable calcium phosphate (Ca-P) cement. J Biomed Mater Res 2002;61:9–18.
19. Comuzzi L, Ooms E, Jansen JA. Injectable calcium phosphate cement as a filler for bone defects around oral implants: An experimental study in goats. Clin Oral Impl Res 2002;13:304–311.
20. Gao H, Ji B, Jägel IL, Arzt E, Fratzl P. Materials become insensitive to flaws at nanoscale: Lessons from nature. Proc Natl Acad Sci USA 2003;100:5597–5600.
21. Fratzl P. Bone fracture. When the cracks begin to show. Nat Mater 2008;7:610–612.
22. Henriksen SS, Ding M, Juhl MV, Theilgaard N, Overgaard S. Mechanical strength of ceramic scaffolds reinforced with

biopolymers is comparable to that of human bone. J Mater Sci: Mater Med 2011;22:1111–1118.
23. Lee SJ, Park YJ, Park SN, Lee YM, Seol YJ, Ku Y, Chung CP. Molded porous poly(L-Lactide) membranes for guided bone regeneration with enhanced effects by controlled growth factor release. J Biomedical Mater Res 2001;55:295–303.
24. Eliaz RE, Kost J. Characterization of a polymeric PLGA injectable implant delivery system for the controlled release of proteins. J Biomed Mater Res 2000;50:388–396.
25. Park TG. Degradation of poly(lactic-co-glycolic acid) microspheres: Effect of copolymer composition. Biomaterials 1995;16: 1123–1130.
26. Holy CE, Dang SM, Davies JE, Shoichet MS. In vitro degradation of a novel poly(lactide-co-glycolide) 75/25 foam. Biomaterials 1999;20:1177–1185.
27. Miao X, Lim WK, Huang X, Chen Y. Preparation and characterization of interpenetrating phased TCP/HA/PLGA composites. Mater Lett 2005;59:4000–4005.
28. Miao X, Tan DM, Li J, Xiao Y, Crawford R. Mechanical and biological properties of hydroxyapatite/tricalcium phosphate scaffolds coated with poly(lactic-co-glycolic acid). Acta Biomater 2008;4: 638–645.
29. Qi X, Ye J, Wang Y. Alginate/poly(lactic-co-glycolic acid)/calcium phosphate cement scaffold with oriented pore structure for bone tissue engineering. J Biomed Mater Res A 2009;89:980–987.
30. Wang X, Ye J, Wang Y, Wu X, Bai B. Control of crystallinity of hydrated products in a calcium phosphate bone cement. J Biomed Mater Res A 2007;81:781–790.
31. Wang XP, Ye JD, Wang YJ. Hydration mechanism of a novel PCCP+DCPA cement system. J Mater Sci: Mater Med 2008;19: 813–816.
32. Shi XT, Wang YJ, Ren L, Zhao NR, Gong YH, Wang D-A. Novel mesoporous silica-based antibiotic releasing scaffold for bone repair. Acta Biomater 2009;5:1697–1707.
33. Takagi S, Chow LC. Formation of macropores in calcium phosphate cement implants. J Mater Sci: Mater Med 2001;12:135–139.
34. Yoshikawa T, Suwa Y, Ohgushi H, Tamai S, Ichijima K. Self setting hydroxyapatite cement as a carrier for bone-forming cells. Biomed Mater Eng 1996;6:345–351.
35. Markovic M, Takagi S, Chow LC. Formation of macropores in calcium phosphate cements through the use of mannitol crystals. Key Eng Mater 2000;192–5:773–776.
36. Del Real RP, Wolke JGC, Vallet-Regi M, Jansen JA. A new method to produce macropores in calcium phosphate cements. Biomaterials 2002;23:3673–3680.
37. Almirall A, Larrecq G, Delgado JA, Martinez S, Planell JA, Ginebra MP. Fabrication of low temperature macroporous hydroxyapatite scaffolds by foaming and hydrolysis of an α-TCP paste. Biomaterials 2004;25:3671–3680.
38. Sarda S, Nilsson M, Balcells M, Fernandez E. Influence of surfactant molecules as air-entraining agent for bone cement macroporosity. J Biomed Mater Res A 2003;65:215–221.
39. Felicity RR, Lesley AC, David MG, Colin AS, Steven MH, Kevin MS. In vitro assessment of cell penetration into porous hydroxyapatite scaffolds with a central aligned channel. Biomaterials 2004;25:5507–5514.
40. Taiyo Y, Kawazoe N, Tateishi T, Chen G. In vitro evaluation of biodegradation of poly(lactic-co-glycolic acid) sponges. Biomaterials 2008;29:3438–3443.
41. Martin RB, Chapman MW, Holmes RE, Sartoris DJ, Shors EC, Gordon JE, Heitter DO, Sharkey NA, Zissimos AG. Effects of bone ingrowth on the strength and noninvasive assessment of a coralline hydroxyapatite material. Biomaterials 1989;10:481–488.
42. Karageorgiou V, Kaplan D. Porosity of 3D biomaterial scaffolds and osteogenesis. Biomaterials 2005;26:5474–5491.
43. Silva MMCG, Cyster LA, Barry JJA, Yangd XB, Oreffo ROC, Grant DM, Scotchford CA, Howdle SM, Shakesheff KM, Rose FR. The effect of anisotropic architecture on cell and tissue infiltration into tissue engineering scaffolds. Biomaterials 2006;27:5909–5917.
44. Rose FR, Cyster LA, Grant DM, Scotchford CA, Howdle SM, Shakesheff KM. In vitro assessment of cell penetration into porous hydroxyapatite scaffolds with a central aligned channel. Biomaterials 2004;25:5507–5514.
45. Chang BS, Lee CK, Hong KS, Youn HJ, Ryu HS, Chung SS, Park KW. Osteoconduction at porous hydroxyapatite with various pore configurations. Biomaterials 2000;21:1291–1298.